Crosstalk between chloroplast protein import and the SUMO system revealed through genetic and molecular investigation

Samuel Watson[1†], Na Li[1], Feijie Wu[2‡], Qihua Ling[1,2‡], R. Paul Jarvis[1,2]*

[1]Department of Plant Sciences, University of Oxford, Oxford OX1 3RB, UK.

[2]Department of Biology, University of Leicester, Leicester LE1 7RH, UK.

[†]Present address: Cambridge Institute for Therapeutic Immunology and Infectious Disease, Jeffrey Cheah Biomedical Centre, University of Cambridge, Cambridge CB2 0AW, UK.

[‡]Present address: National Key Laboratory of Plant Molecular Genetics, CAS Centre for Excellence in Molecular Plant Sciences, Institute of Plant Physiology and Ecology, Shanghai Institutes for Biological Sciences, Chinese Academy of Sciences, Shanghai, China.

*For correspondence: paul.jarvis@plants.ox.ac.uk

Abstract

The chloroplast proteome contains thousands of different proteins that are encoded by the nuclear genome. These proteins are imported into the chloroplast via the action of the TOC translocase and associated downstream systems. Our recent work has revealed that the stability of the TOC complex is dynamically regulated via the ubiquitin-dependent chloroplast-associated protein degradation (CHLORAD) pathway. Here, we demonstrate that the stability of the TOC complex is also regulated by the SUMO system. *Arabidopsis* mutants representing almost the entire SUMO conjugation pathway can partially suppress the phenotype of *ppi1*, a pale yellow mutant lacking the Toc33 protein. This suppression is linked to increased stability of TOC proteins and enhanced chloroplast development. In addition, we demonstrate using molecular and biochemical experiments that the SUMO system directly targets TOC proteins. Thus, we have identified a regulatory link between the SUMO system and chloroplast protein import.

Introduction

The chloroplast is a membrane-bound organelle that houses photosynthesis in all green plants (Jarvis and Lopez-Juez, 2013). Chloroplasts have an unusual evolutionary history – they are the integrated descendants of a free-living cyanobacterial ancestor that entered the eukaryotic lineage via endosymbiosis. Although chloroplasts retain small genomes, almost all of the proteins required for chloroplast development and function are now encoded by the central, nuclear genome (Jarvis, 2008). These proteins must be imported into the organelle after synthesis in the cytosol, and this import is mediated by the coordinate action of the TOC and TIC complexes (the translocons at the outer and inner envelope membranes of chloroplasts) (Jarvis, 2008).

The TOC complex contains three major components: the Omp85 (outer membrane protein, 85 kD)-related protein, Toc75, which serves as a membrane channel (Schnell et al., 1994; Tranel et al., 1995), and two GTPase-domain receptor proteins, Toc33 and Toc159 (Hirsch et al., 1994; Kessler et al., 1994; Perry and Keegstra, 1994; Jarvis et al., 1998; Jarvis, 2008). Toc33 and Toc159 project out into the cytosol and bind incoming preproteins.

The key components of the TOC complex were identified more than two decades ago (Hirsch et al., 1994; Kessler et al., 1994; Schnell et al., 1994; Tranel et al., 1995; Jarvis, 2008). However, the regulation of the activity and stability of the complex was, until recently, poorly understood. Major insights came from a forward genetic screen for suppressors of the pale yellow Toc33 mutant, *ppi1* (Ling et al., 2012). As a result of this screen, a novel RING-type E3 ubiquitin ligase, SP1 (SUPPRESSOR OF PPI1 LOCUS 1), was identified. A series of *sp1* mutants were shown to partially suppress the phenotypic defects of *ppi1* with respect to chlorosis, chloroplast development, and chloroplast protein import. In addition, SP1 function was shown to promote plastid interconversion events (for example, the development of the chloroplast from its precursor organelle, the etioplast). Later work demonstrated that SP1 function is also important for abiotic stress tolerance, by enabling optimisation of the organellar proteome via protein import regulation (Ling and Jarvis, 2015). Thus, through SP1, the ubiquitin-proteasome system promotes TOC complex degradation and reconfiguration in response to developmental and/or environmental stimuli.

Ubiquitinated TOC proteins are extracted from the chloroplast outer envelope membrane and degraded in the cytosol. Recent work identified two proteins that physically associate with SP1 and promote the membrane extraction of TOC proteins (Ling et al., 2019). These are SP2, an Omp85-type β-barrel channel protein that was identified in the same genetic screen as SP1, and Cdc48, a well-characterised cytosolic AAA+ chaperone ATPase that provides the motive force for the extraction of proteins from the chloroplast outer envelope. The three proteins – SP1, SP2 and Cdc48 – together define a new pathway for the ubiquitination, membrane extraction, and degradation of chloroplast outer envelope proteins, which has been named chloroplast-associated protein degradation, or CHLORAD. In addition to CHLORAD, there exist cytosolic ubiquitin-dependent systems that also contribute to chloroplast biogenesis, by regulating the levels of unimported preproteins (Lee et al., 2009; Grimmer et al., 2020), and by controlling the stability of the Toc159 receptor prior to its integration into the outer envelope membrane (Shanmugabalaji et al., 2018).

The discovery of SP1 and the CHLORAD pathway demonstrated that the TOC complex is not static but, instead, can be rapidly ubiquitinated and degraded in response to developmental and environmental stimuli. To complement this work, we decided to explore whether the TOC complex is also regulated by the SUMO system. This work was motivated by the results of a high-throughput screen for SUMO substrates in *Arabidopsis* (Elrouby and Coupland, 2010). This screen suggested that Toc159, a key component of the TOC complex, is a SUMO substrate. SUMOylation is intricately

involved in plant development and stress adaptation, and so we were interested to determine whether the TOC complex is targeted by the SUMO target, and whether this SUMOylation is functionally important. As crosstalk between the SUMO system and the ubiquitin-proteasome system is common, we reasoned that answering these questions might provide insights into the regulation of SP1 and the CHLORAD pathway.

To explore the relationship between chloroplast protein import and the SUMO system, we carried out a comprehensive series of genetic, molecular and biochemical experiments. Mutants representing most components of the *Arabidopsis* SUMO pathway were found to partially suppress the phenotype of the chlorotic Toc33 null mutant, *ppi1*, with respect to leaf chlorophyll accumulation, chloroplast development, and TOC protein abundance. Conversely, overexpression of either *SUMO1* or *SUMO3* enhanced the severity of the *ppi1* phenotype. Moreover, the E2 SUMO conjugating enzyme, SCE1, was found to physically interact with the TOC complex in bimolecular fluorescence complementation experiments; and TOC proteins were seen to physically associate with SUMO proteins in immunoprecipitation assays. In combination, our data conclusively demonstrate significant crosstalk between the SUMO system and chloroplast protein import, and emphasise the complexity of the regulation of the TOC translocase.

Results

The E2 SUMO conjugating enzyme mutant, *sce1-4*, and the E3 SUMO ligase mutant, *siz1-4*, partially suppress the Toc33 mutant, *ppi1*

Two key components of the CHLORAD pathway, SP1 and SP2, were identified in a forward genetic screen for suppressors of the *Arabidopsis* Toc33 null mutant, *ppi1* (Ling et al., 2012; Ling et al., 2019). Both *sp1* and *sp2* mutants can partially suppress *ppi1* with respect to chlorophyll accumulation, chloroplast development, and TOC protein abundance. Thus, in an effort to determine whether the TOC complex is targeted by the SUMO system, we obtained several *Arabidopsis* SUMO system mutants and crossed them with *ppi1*, and then carefully examined the phenotypes of the resulting double mutants.

First, we analysed *sce1-4*, an E2 SUMO conjugating enzyme mutant. SCE1 is the only known E2 SUMO conjugating enzyme in *Arabidopsis* and it is essential (Saracco et al., 2007). The *sce1-4* mutant shows a moderate reduction in the expression of SCE1 but displays no obvious phenotypic defects under steady-state conditions (Saracco et al., 2007). The *ppi1 sce1-4* double mutant was phenotypically characterised, and, intriguingly, it appeared greener than the *ppi1* single mutant when grown on soil (Figure 1A). This was linked to a moderate increase in leaf chlorophyll concentration (Figure 1B). Next, we asked whether the phenotypic suppression observed in *ppi1 sce1-4* was linked to changes in the development of chloroplasts. The chloroplasts of *ppi1 sce1-4* were visualised via transmission electron microscopy. Interestingly, the chloroplasts of the *ppi1 sce1-4* double mutant appeared larger and better developed than those of the *ppi1* control (Figure 1C). The transmission electron micrographs were quantitatively analysed, and the *ppi1 sce1-4* chloroplasts were indeed found to be significantly larger than those of *ppi1* (Figure 1D), with larger, more interconnected thylakoidal granal stacks (Figures 1E and 1F).

SUMO conjugation is usually dependent on the action of E3 SUMO ligases. In *Arabidopsis*, the best characterised E3 SUMO ligase is SIZ1 (Kurepa et al., 2003; Miura et al., 2005; Saracco et al., 2007). SIZ1 is not essential, but null mutants display severely dwarfed phenotypes. In order to include SIZ1 in our genetic analysis, it was necessary to identify a new mutant that had a less severe phenotype than the null mutants. To this end, we obtained two new T-DNA insertion alleles, and named them

116 *siz1-4* and *siz1-5.* One of the mutants, *siz1-4*, showed a milder phenotype than published mutants –
117 it showed only moderate growth retardation when grown to maturity. The two *siz1* mutants were
118 crossed with *ppi1* and the resulting double mutants were phenotypically characterised. Both the
119 *ppi1 siz1-4* and the *ppi1 siz1-5* double mutants appeared greener than the *ppi1* control when grown
120 on soil (Figure 1G). In addition, the *ppi1 siz1-4* double mutant showed a dramatic increase in leaf
121 chlorophyll concentration relative to *ppi1* (Figure 1H). Next, we asked if the phenotypic suppression
122 observed in *ppi1 siz1-4* was linked to changes in the abundance of TOC proteins. Protein samples
123 were taken from the mature leaves of the double mutant (and relevant control plants) and resolved
124 via immunoblotting. Intriguingly, the *ppi1 siz1-4* double mutant displayed a robust increase in the
125 abundance of Toc159 and Toc75, two core components of the TOC complex (Figure 1I). In contrast,
126 the abundance of Tic110 and Tic40, two TIC complex proteins which were included here as controls,
127 was unaffected.

128 **The suppression effects mediated by the SUMO system mutants are specific**

129 A large number of proteins are subject to SUMOylation in *Arabidopsis*; however, the SUMO system is
130 encoded by only a small number of genes. Thus, SUMO system mutants have highly pleiotropic
131 molecular and physiological phenotypes. We therefore asked whether the partial suppression of
132 *ppi1* by SUMO system mutants was specific to the *ppi1* background. To address this question, we
133 crossed *sce1-4* with two pale, TIC complex associated mutants – *tic40-4* and *hsp93-V-I*. These
134 mutants are chlorotic due to defects in protein import across the chloroplast inner membrane and in
135 this respect are highly similar to *ppi1* (Kovacheva et al., 2005). Significantly, the resulting double
136 mutants, *tic40-4 sce1-4* and *hsp93-V-I sce1-4*, were indistinguishable from their respective single
137 mutant controls (*tic40-4* and *hsp93-V-I*) (Figures 2A and 2C). Moreover, the double mutants did not
138 display increases in leaf chlorophyll accumulation relative to the single mutant controls (Figures 2B
139 and 2D). Therefore, we concluded that the suppression effects observed in *ppi1 sce1-4* were highly
140 background-specific and were tightly associated with the TOC complex.

141 Next, we asked whether the *sce1-4* and *siz1-4* single mutants display an increase in chlorophyll
142 concentration even in the wild-type background. However, neither mutant appeared greener than
143 wild-type plants (Figures 2E and 2G) or displayed an increase in leaf chlorophyll concentration
144 (Figures 2F and 2H). This was particularly noteworthy in the case of *siz1-4*, as the *ppi1 siz1-4* double
145 mutant displayed near complete phenotypic suppression with respect to leaf chlorophyll
146 concentration (Figure 1H). Thus, we concluded that the suppression effects mediated by both
147 mutants, as shown in Figure 1, were synthetic phenotypes specific to the *ppi1* background.

148 **BiFC analysis reveals that SCE1 physically interacts with TOC proteins**

149 Our reverse genetic experiments revealed a genetic link between the E2 SUMO conjugating enzyme,
150 SCE1, and protein import across the chloroplast outer membrane. To determine whether SCE1
151 directly interacts with the TOC complex, bimolecular fluorescence complementation (BiFC)
152 experiments were performed in *Arabidopsis* protoplasts. To this end, the *SCE1* coding sequence was
153 inserted into a vector that C-terminally appends the N-terminal half of YFP (nYFP). This construct was
154 co-expressed with various other constructs encoding TOC proteins bearing the complementary, C-
155 terminal moiety of the YFP protein (cYFP), appended C-terminally. In this system, protein-protein
156 interactions are inferred via the detection of a YFP signal, caused by the nYFP and cYFP fragments
157 coming together to reconstitute a functional YFP protein.

158 Strikingly, SCE1-nYFP was found to physically associate with all tested TOC proteins – Toc159-cYFP,
159 Toc132-cYFP, Toc34-cYFP and Toc33-cYFP (Figure 3). Moreover, these interactions were

160 concentrated at the periphery of the chloroplasts, placing them in an appropriate subcellular context
161 for the *in situ* regulation of the chloroplast protein import machinery. Conversely, SCE1-nYFP was
162 not found to physically associate with the negative control protein ΔOEP7-cYFP. This protein
163 comprises the transmembrane domain of plastid protein OEP7 fused to the cYFP fragment. The
164 transmembrane domain of OEP7 is sufficient to efficiently target the full-length YFP protein to the
165 chloroplast outer membrane (Lee et al., 2001); thus ΔOEP7-cYFP serves as a location-specific
166 negative control.

167 **Manipulating the expression of three SUMO isoforms alters the phenotypic severity of *ppi1***

168 The preceding genetic and molecular experiments revealed a clear link between the SUMO system
169 and chloroplast protein import, implying that TOC proteins are SUMOylated. We therefore decided
170 to carry out a series of experiments to assess for genetic interactions between genes encoding
171 SUMO proteins and *ppi1*. There are three major SUMO isoforms in *Arabidopsis* – SUMO1, SUMO2,
172 and SUMO3. The *SUMO1* and *SUMO2* genes are expressed at a relatively high level throughout the
173 plant and are largely functionally redundant (Saracco et al., 2007; van den Burg et al., 2010). In
174 addition, they are highly similar to each other in terms of amino acid sequence (Saracco et al., 2007).
175 In contrast, at steady state, *SUMO3* is expressed at a relatively low level throughout the plant, while
176 the SUMO3 amino acid sequence is significantly divergent with respect to the other two SUMO
177 isoforms (van den Burg et al., 2010).

178 First, we analysed *SUMO1* and *SUMO2*. We obtained *sum1-1* and *sum2-1*, two previously
179 characterised *Arabidopsis* null mutants (Saracco et al., 2007), and crossed them with *ppi1*. To
180 account for the functional redundancy between these two genes, we also sought a *ppi1 sum1-1*
181 *sum2-1* triple mutant. However, as *SUMO1* and *SUMO2* are collectively essential, *ppi1 sum1-1 sum2-*
182 *1* plants that were homozygous with respect to *ppi1* and *sum2-1*, but heterozygous with respect to
183 the *sum1-1* mutation, were selected from a segregating population. The double and triple mutants
184 were phenotypically characterised, and all three appeared larger and greener than the *ppi1* control
185 plants (Figure 4A). Moreover, the double and triple mutants showed corresponding increases in leaf
186 chlorophyll concentration, with the triple mutant showing a larger increase than the double mutants
187 (Figure 4B). Therefore, we concluded that the *sum1-1* and *sum2-1* mutants can additively suppress
188 the phenotype of *ppi1*.

189 To complement the above-described experiment, we generated transgenic plants overexpressing
190 *SUMO1* in the *ppi1* background. The *SUMO1* coding sequence was cloned into a vector carrying a
191 strong, constitutive promotor (cauliflower mosaic virus 35S) upstream of the cloning site. The
192 resulting construct was stably introduced into the *ppi1* background via *Agrobacterium*-mediated
193 transformation. Two lines carrying a single, homozygous transgene insert were identified and taken
194 forward for analysis. The overexpression of *SUMO1* was confirmed in both lines via semi-
195 quantitative RT-PCR (Figure 4 supplement, panel A). Significantly, both lines displayed an
196 accentuation of the *ppi1* phenotype – the plants were significantly smaller and paler than the *ppi1*
197 control plants (Figure 4C), and showed decreases in leaf chlorophyll concentration (Figure 4D).

198 Next, we turned our attention to *SUMO3*. We obtained *sum3-1*, a previously characterised null
199 mutant (van den Burg et al., 2010), and crossed it with *ppi1*. The resulting double mutant was
200 phenotypically characterised, and, interestingly, it did not appear obviously different from the *ppi1*
201 control (Figure 4E). Correspondingly, it did not display any clear increase in leaf chlorophyll
202 concentration relative to *ppi1* (Figure 4F). To complement this experiment, we generated transgenic
203 plants overexpressing *SUMO3* in the *ppi1* background, using the approach described above, and a
204 line carrying a single, homozygous insert was identified and taken forward for analysis. The

205 overexpression of *SUMO3* was confirmed via semi-quantitative RT-PCR (Figure 4 supplement, panel
206 B). Interestingly, the transgenic plants showed a striking increase in the severity of the *ppi1*
207 phenotype – the plants were severely dwarfed and paler than the *ppi1* control (Figure 4G), and
208 displayed a significant decrease in leaf chlorophyll accumulation (Figure 4H). These findings are
209 particularly noteworthy when considered alongside a previous report which explored the
210 consequences of overexpressing *SUMO3* in wild-type plants (van den Burg et al., 2010). In that
211 previous work, *SUMO3* overexpression was not found to alter the appearance of the transgenic
212 plants, which implies a degree of specificity in the phenotypic accentuation observed here.

213 **Biochemical analysis reveals SUMOylation of TOC proteins *in vivo***

214 The genetic and molecular experiments described thus far strongly suggested that TOC proteins are
215 SUMOylated. However, to our knowledge, conclusive evidence that chloroplast-resident proteins are
216 SUMOylated is currently lacking. Therefore, to investigate whether chloroplast proteins may be
217 SUMOylated, we isolated chloroplasts from seedlings by cell fractionation, and analysed them by
218 anti-SUMO immunoblotting. For this analysis, we employed a proven commercial antibody against
219 SUMO1, which is one of the most abundant SUMO isoforms in *Arabidopsis* making it more tractable
220 for analysis, and which furthermore is known to accumulate in response to heat and other stresses
221 (Kurepa et al., 2003; van den Burg et al., 2010). With the goal of enhancing the detection of
222 SUMOylated proteins in our samples, we subjected some of the seedlings to heat shock before
223 chloroplast isolation and/or treatment with 10 mM N-ethylmaleimide (NEM) during chloroplast
224 isolation; NEM is a potent inhibitor of SUMO-specific proteases (Hilgarth and Sarge, 2005).
225 Importantly, we detected protein SUMOylation in the isolated chloroplast samples, and this
226 SUMOylation was increased by NEM treatment (Figure 5 supplement 1).

227 Next, we sought to determine whether TOC proteins are SUMOylated. To test this idea directly, a
228 number of biochemical experiments were performed. In the first of these, the *SCE1* coding sequence
229 was cloned into a vector that appends a C-terminal YFP tag (Karimi et al., 2002). The resulting SCE1-
230 YFP construct expressed well and showed the expected nucleocytoplasmic fluorescence pattern
231 when transiently expressed in *Arabidopsis* protoplasts (Figure 5 supplement 2, panel A). Thus, larger
232 numbers of protoplasts were transfected with the SCE1-YFP construct, or a YFP-HA negative control
233 construct, and the transfected cells were solubilised and incubated with YFP-Trap magnetic beads.
234 After incubation, the beads were magnetically separated from the lysate, then boiled in loading
235 buffer to release bound proteins. The eluted proteins, along with total lysate and flow-through
236 samples, were analysed by immunoblotting. The YFP-HA and SCE1-YFP fusion proteins both showed
237 robust expression, and strong recovery in the IP fractions (Figure 5A). By analysing the samples using
238 a range of other antibodies, the SCE1-YFP fusion protein was found to be associated with native
239 Toc159 and Toc132 but not with the negative control proteins Tic110 or Tic40 (Figure 5A).
240 Conversely, YFP-HA did not associate with any of the tested proteins.

241 In the second experiment, we cloned the *SUMO1*, *SUMO2*, and *SUMO3* coding sequences into a
242 vector that appends an N-terminal YFP tag (Karimi et al., 2002), a modification which previous
243 studies have shown to be tolerated (Ayaydin and Dasso, 2004). All three constructs expressed well
244 and showed the expected nucleocytoplasmic fluorescence pattern when transiently expressed in
245 protoplasts (Figure 5 supplement 2, panel B). The three constructs were expressed in parallel in
246 protoplasts, as well as the YFP-HA negative control construct. As in the previous experiment,
247 solubilised protoplasts were subjected to YFP-Trap immunoprecipitation, and protein samples were
248 analysed by immunoblotting. Remarkably, all three YFP-SUMO proteins were found to physically
249 associate with Toc159, although YFP-SUMO3 clearly bound Toc159 with the greatest affinity (Figure
250 5B). Moreover, inspection of an extended exposure of the anti-YFP blot revealed a number of higher

251 molecular weight bands that we interpret to be SUMO adducts and indicative of the functionality of
252 the fusions (Figure 5 supplement 3). In contrast with the SUMO fusions, the YFP-HA negative control
253 did not associate with Toc159; and none of the four SUMO fusion proteins physically associated with
254 Tic40, a negative control protein (Figure 5B).

255 The immunoprecipitation experiment described above identified SUMO3 as having the highest
256 affinity for Toc159. To extend our analysis of SUMO3 to include another TOC protein, and to provide
257 more direct evidence for TOC protein SUMOylation, the experiment was repeated with
258 modifications, as follows. Protoplasts were co-transfected with YFP-SUMO3 and Toc33-HA, or YFP-
259 HA and Toc33-HA; in each case, the transient overexpression of Toc33 was done to aid detection of
260 this component and its adducts. The construct pairs were co-expressed in protoplasts, and then the
261 samples were subjected to YFP-Trap immunoprecipitation analysis, as described earlier. In
262 accordance with the Toc159 result (Figure 5B), YFP-SUMO3, but not YFP-HA, was found to physically
263 associate with Toc33-HA (Figure 5C). Moreover, bands of the exact expected molecular weight of
264 Toc33-HA bearing one or two YFP-SUMO3 moieties (75 and 114 kDa) were also detected. These
265 bands were accompanied by a high molecular weight smear at the top of the immunoblot, which is
266 indicative of complex, multisite or chain SUMOylation.

267 Discussion

268 This work has revealed a genetic and molecular link between the SUMO system and chloroplast
269 protein import. The genetic experiments demonstrated that SUMO system mutants can suppress the
270 phenotype of the Toc33 mutant, *ppi1*, and the molecular and biochemical experiments indicated
271 that TOC proteins associate with key SUMO system proteins and are SUMOylated. Visible
272 suppression effects observed in the *ppi1* / SUMO system double mutants were linked to
273 improvements in chloroplast development and enhanced accumulation of key TOC proteins.
274 Importantly, each core TOC protein, including all of those analysed in this study, was predicted with
275 high probability to have one or more SUMOylation sites (Table 1) (Zhao et al., 2014; Beauclair et al.,
276 2015).

277 The *ppi1* suppression effects described here are remarkably similar to those mediated by the *sp1*
278 and *sp2* mutants (Ling et al., 2012; Ling et al., 2019). Like *sp1* and *sp2*, SUMO system mutants can
279 partially suppress *ppi1* with respect to chlorophyll concentration, TOC protein accumulation, and
280 chloroplast development. This similarity suggests that SUMOylation may regulate the activity of the
281 CHLORAD pathway. This is an attractive hypothesis, as both SUMOylation and the CHLORAD
282 pathway are activated by various forms of environmental stress (Kurepa et al., 2003; Ling and Jarvis,
283 2015; Ling et al., 2019). One possibility is that SUMOylation of TOC proteins promotes their
284 CHLORAD-mediated degradation. Certainly, the ability to carry out SUMOylation is negatively
285 correlated with the stability of TOC proteins in the context of the developed plants studied here.
286 However, it should be kept in mind that SUMOylation can both promote and antagonise the effects
287 of ubiquitination, in different situations (Desterro et al., 1998; Ahner et al., 2013; Liebelt and
288 Vertegaal, 2016); and so our results do not preclude the possibility that SUMOylation may have
289 different consequences for chloroplast biogenesis in other contexts. The Toc159 receptor is
290 regulated by SP1 when integrated into the outer envelope membrane (Ling et al., 2012; Ling et al.,
291 2019), but by a different E3 ligase when it exists as a cytosolic precursor during the earliest stages of
292 development before germination (Shanmugabalaji et al., 2018). Thus, regulation by SUMOylation
293 might be similarly different in these two distinct developmental contexts.

294 The precise mechanisms underpinning the observed negative regulation of the TOC apparatus by
295 SUMOylation are currently unknown. One possibility is that the SUMOylation of TOC proteins

296 promotes their association with SP1. SUMOylation can modify protein-protein interactions, and
297 some RING-type E3 ubiquitin ligases specifically recognise SUMOylated substrates (Sriramachandran
298 and Dohmen, 2014). However, these SUMO-targeted ubiquitin ligases (STUbLs) typically contain
299 SUMO-interacting motifs (SIMs) which guide the ligases to SUMO proteins conjugated to their
300 substrates, and these are not apparent in SP1 (data not shown) (Zhao et al., 2014). However, SP1
301 forms a complex with SP2 and very likely additional cofactors, and these could hypothetically
302 provide a SUMO binding interface. Another possibility is that SUMOylation could be involved in the
303 recruitment of Cdc48 from the cytosol. Two important Cdc48 cofactors are Ufd1 and Npl4, and the
304 former contains a SUMO-interacting motif which can guide Cdc48 to SUMOylated proteins (Nie et
305 al., 2012; Baek et al., 2013). Moreover, the SUMO-mediated recruitment of Cdc48 has important
306 roles in the maintenance of genome stability in yeast (Bergink et al., 2013).

307 The biochemical experiments described herein indicate that, of the three SUMO isoforms tested,
308 SUMO3 binds TOC proteins with the highest affinity. However, there is an apparent incongruence
309 between the results of these experiments and the results of the genetic experiments. While the
310 *sum1-1* and *sum2-1* mutants were found to additively suppress *ppi1*, the *sum3-1* mutant did not
311 suppress *ppi1*. At face value, this seems puzzling; however, it can be explained by the relative
312 abundance of the three SUMO proteins *in planta*. SUMO1 and SUMO2 are highly abundant relative
313 to SUMO3, which is, at steady state, very weakly abundant (van den Burg et al., 2010). The
314 immunoprecipitation data shown in Figure 5B indicated that SUMO1 and SUMO2 can weakly
315 interact with Toc159, and so it is likely that these two isoforms can compensate for the loss of
316 SUMO3 in the *sum3-1* mutant. Although SUMO3 associates with TOC proteins with the highest
317 affinity, the higher abundance of the other two SUMO proteins may facilitate such compensation.

318 It is now well established that the regulation of chloroplast protein import has critical roles in plant
319 development and stress acclimation (Sowden et al., 2018; Watson et al., 2018). Here, we
320 demonstrate regulatory crosstalk between the SUMO system and chloroplast protein import, and
321 present results which are consistent with a model in which SUMOylation modulates the activity or
322 effects of the CHLORAD pathway. The precise nature of the links between these two critically
323 important control systems will be the subject of future investigation.

324 Materials and methods

325 Plant material and growth conditions

326 All *Arabidopsis thaliana* plants used in this work were of the Columbia-0 (Col-0) ecotype. The
327 mutants used in almost all of the analyses (*ppi1*, *sce1-4*, *sum1-1*, *sum2-1*, *sum3-1*, *hsp93-V-I*, *tic40-4*)
328 have been described previously (Jarvis et al., 1998; Kovacheva et al., 2005; Saracco et al., 2007; van
329 den Burg et al., 2010). The *siz1-4* (SAIL_805_A10) and *siz1-5* (SALK_111280) mutants were obtained
330 from the Salk Institute Genomic Analysis Laboratory (SIGnAL) (Alonso et al., 2003), via the
331 Nottingham *Arabidopsis* Stock Centre (NASC). Each line was verified via PCR genotyping (see Table 2
332 for primer sequences) and phenotypic analysis (including the double and triple mutants).

333 In most experiments, plants were grown on soil (80% (v/v) compost (Levington M2), 20% (v/v)
334 vermiculite (Sinclair Pro, medium particle size)). However, where plants were grown for selection of
335 transformants or for chloroplast isolation, seeds were surface sterilised and sown on petri plates
336 containing Murashige-Skoog (MS) agar medium. The plates were stored at 4°C for 48 hours before
337 being transferred to a growth chamber. Both soil-grown and plate-grown plants were kept in a
338 growth chamber (Percival Scientific) under long-day conditions (16 hours light, 8 hours dark). The

339 light intensity was approximately 120 µE m^{-2} s^{-1}, the temperature was held constant at 20°C, and the
340 humidity was held constant at approximately 70% (relative humidity).

341 **Chlorophyll measurements**

342 Chlorophyll measurements were taken from mature rosette leaves in each instance. A handheld
343 Konica-Minolta SPAD-502 meter was used to take each measurement, and the raw values were
344 converted into chlorophyll concentration values (nmol/mg tissue) via published calibration
345 equations (Ling et al., 2011).

346 **Chloroplast isolation and protein extraction**

347 Chloroplasts were isolated from 14-day-old, plate-grown seedlings as described previously (Flores-
348 Pérez and Jarvis, 2017). Some of the seedlings were heat-shocked immediately prior to chloroplast
349 isolation. To do this, the plates containing the seedlings were wrapped in clingfilm and placed into a
350 water bath (42°C for 30 seconds). Protein samples were prepared from the isolated chloroplasts by
351 extraction using SDS-PAGE sample buffer, as well as from whole 14-day-old seedlings as previously
352 described (Kovacheva et al., 2005). In some cases, the samples were treated with 10 mM N-
353 ethylmaleimide (Hilgarth and Sarge, 2005); this was added directly to the protein extraction buffer
354 (whole seedling samples), or to the chloroplast isolation buffer following polytron homogenization
355 and all subsequent buffers (chloroplast samples).

356 **Plasmid constructs**

357 The constructs used in the BiFC experiments were generated as follows. The coding sequences of
358 *SCE1*, *SIZ1*, *TOC159*, *TOC132*, *TOC34*, *TOC33* and *SFR2* were PCR amplified from wild-type cDNA (see
359 Table 2 for primer sequences). In the case of *ΔOEP7*, the first 105 base pairs of the *OEP7* coding
360 sequence were amplified; this encodes a truncated sequence which is sufficient to efficiently target
361 the full-length YFP protein to the chloroplast outer envelope membrane (Lee et al., 2001). The
362 inserts were cloned into one of the following complementary vectors: pSAT4(A)-nEYFP-N1 (*SCE1*),
363 pSAT4-cEYFP-C1-B (*TOC159*, *TOC132*, *TOC34*, *TOC33*), or pSAT4(A)-cEYFP-N1 (*ΔOEP7*, *SFR2*), which
364 were described previously (Tzfira et al., 2005; Citovsky et al., 2006).

365 The constructs used in the immunoprecipitation experiments were generated as follows. The coding
366 sequences of *SCE1*, *SUMO1*, *SUMO2* and *SUMO3* were PCR amplified from wild-type cDNA using
367 primers bearing 5' attB1 and attB2 adaptor sequences (see Table 2 for primer sequences). The
368 amplicons were then cloned into pDONR221 (Invitrogen), a Gateway entry vector. The inserts from
369 the resulting entry clones were then transferred to one of two destination vectors: p2GWY7 (*SCE1*)
370 or p2YGW7 (*SUMO1*, *SUMO2*, *SUMO3*); the former appends a C-terminal YFP tag to its insert, and
371 the latter appends an N-terminal YFP tag to its insert (Karimi et al., 2002; Karimi et al., 2005). The
372 Toc33-HA and YFP-HA constructs have been described previously (Ling et al., 2019).

373 The constructs used to generate transgenic plants were generated as follows. The coding sequences
374 of *SUMO1* and *SUMO3* were PCR amplified from wild-type cDNA using primers bearing 5' attB1 and
375 attB2 adaptor sequences (see Table 2 for primer sequences). The inserts were then cloned into
376 pDONR201 (Invitrogen), a Gateway entry vector. The inserts from the resulting entry clones were
377 then transferred to the pH2GW7 binary destination vector (Karimi et al., 2002; Karimi et al., 2005).

378 **Transient expression assays**

379 Protoplasts were isolated from mature rosette leaves of wild-type *Arabidopsis* plants and
380 transfected in accordance with an established method (Wu et al., 2009; Ling et al., 2012). In the BiFC

381 experiments, 100 µL protoplast suspension (containing approximately 10^5 protoplasts) was
382 transfected with 5 µg plasmid DNA; and in the immunoprecipitation experiments, 600 µL protoplast
383 suspension (containing approximately 6×10^5 protoplasts) was transfected with 30 µg plasmid DNA.
384 In both cases, the samples were analysed after 15-18 hours.

385 **Stable plant transformation**

386 Transgenic lines carrying the *SUMO1-OX* or *SUMO3-OX* constructs were generated via
387 *Agrobacterium*-mediated floral dip transformation (Clough and Bent, 1998). Transformed plants (T_1
388 generation) were selected on MS medium containing phosphinothricin. Multiple T_2 families were
389 analysed in each case, and lines bearing a single T-DNA insertion were taken forward for further
390 analysis. Transgene expression was analysed by semi-quantitative RT-PCR as described previously
391 (Kasmati et al., 2011) (see Table 2 for primer sequences).

392 **Transmission electron microscopy**

393 Transmission electron micrographs were recorded using mature rosette leaves as previously
394 described (Huang et al., 2011). Images were taken from three biological replicates (different leaves
395 from different individual plants), and at least 10 images were taken per replicate. The images were
396 analysed using ImageJ (Schneider et al., 2012). The freehand tool was used to measure the plan area
397 of the chloroplasts. For this, between 9 and 28 chloroplasts were analysed for each biological
398 replicate (i.e., for each plant), and then an average value for each replicate was calculated and used
399 for statistical comparisons. The analysis of chloroplast ultrastructure was performed as in previous
400 work (Huang et al., 2011). For this, between 3 and 8 chloroplasts were analysed per biological
401 replicate, and the data were processed as above.

402 **BiFC experiments**

403 The BiFC experiments were carried out as described previously (Ling et al., 2019). Protoplasts were
404 co-transfected with two constructs encoding fusion proteins bearing complementary fragments of
405 the YFP protein (nYFP and cYFP) (Citovsky et al., 2006). After transfection and overnight incubation,
406 the protoplasts were imaged using a Zeiss LSM 510 META laser-scanning confocal micro-scope (Carl
407 Zeiss) and the presence and distribution, or absence, of a YFP signal was recorded.

408 **Immunoblotting and immunoprecipitation**

409 Protein extraction and immunoblotting were performed as described in previously (Kovacheva et al.,
410 2005). Total protein samples extracted from 30-50 mg leaf tissue were typically analysed. To detect
411 proteins, we used an anti-SUMO1 antibody (Ab5316, Abcam), an anti-Toc75-III-3 antibody (Kasmati
412 et al., 2011), an anti-Toc159 antibody (Bauer et al., 2000), an anti-Tic110 antibody (Inaba et al.,
413 2005), an anti-Tic40 antibody (Kasmati et al., 2011), and an anti-green fluorescent protein antibody
414 (Sigma). In most cases, the secondary antibody used was anti-rabbit immunoglobulin G (IgG)
415 conjugated with horseradish peroxidase (Santa Cruz Biotechnology); and protein bands were
416 visualised via chemiluminescence using an ECL Plus Western blotting detection kit (GE Healthcare)
417 and an LAS-4000 imager (Fujifilm). However, in the case of Figure 5 supplement 1, the secondary
418 antibody was anti-rabbit IgG conjugated with alkaline phosphatase (Sigma), and the membrane was
419 incubated with BCIP/NBT chromogenic substrate (Sigma).

420 The immunoprecipitation (IP) experiments were also carried out as described previously (Ling et al.,
421 2019). Constructs encoding YFP-conjugated fusion proteins (YFP-HA, SCE1-YFP, YFP-SUMO1, YFP-
422 SUMO2, YFP-SUMO3) were transiently expressed in protoplasts. In some cases, the constructs were
423 co-expressed with a construct encoding Toc33-HA. The protoplasts were solubilised using IP buffer

424 containing 1% Triton X-100, and the resulting lysates were incubated with GFP-Trap beads
425 (Chromotek). After four washes in IP buffer, the protein samples were eluted by boiling in SDS-PAGE
426 loading buffer, and then analysed by immunoblotting.

427 **Statistical analysis**

428 The data from each experiment were analysed in R. In most cases, two-tailed T-tests were
429 performed. However, in one case, a one-way ANOVA was performed in conjunction with a Tukey
430 HSD test (as indicated in the figure legend). Asterisks in the figures indicate the level of significance,
431 as follows: *, $p<0.05$; **, $p<0.01$; ***, $p<0.001$; ****, $p<0.0001$; *****, $p<0.00001$.

432 **SUMO site prediction**

433 The amino acid sequences of Toc159, Toc132, Toc120, Toc90, Toc75, Toc33 and Toc34 were
434 retrieved from The *Arabidopsis* Information Resource (TAIR) website (Berardini et al., 2015). The
435 GPS-SUMO algorithm was applied to all seven sequences (http://sumosp.biocuckoo.org/online.php)
436 (Zhao et al., 2014). The 'high stringency' setting was applied. The *p*-values were generated by the
437 GPS-SUMO algorithm, and hits that were accompanied by *p*-values exceeding $p=0.05$ were manually
438 removed. The JASSA algorithm was also applied to all seven amino acid sequences
439 (http://www.jassa.fr/index.php) (Beauclair et al., 2015). In this case, the 'high cut-off' setting was
440 applied. The GPS-SUMO and JASSA algorithms use fundamentally different methodologies (Chang et
441 al., 2018).

442 References and notes

443 **Ahner, A., Gong, X., and Frizzell, R.A.** (2013). Cystic fibrosis transmembrane conductance regulator
444 degradation: cross-talk between the ubiquitylation and SUMOylation pathways. FEBS Journal
445 **280,** 4430-4438.
446 **Alonso, J.M., Stepanova, A.N., Leisse, T.J., Kim, C.J., Chen, H., Shinn, P., Stevenson, D.K.,**
447 **Zimmerman, J., Barajas, P., Cheuk, R., Gadrinab, C., Heller, C., Jeske, A., Koesema, E.,**
448 **Meyers, C.C., Parker, H., Prednis, L., Ansari, Y., Choy, N., Deen, H., Geralt, M., Hazari, N.,**
449 **Hom, E., Karnes, M., Mulholland, C., Ndubaku, R., Schmidt, I., Guzman, P., Aguilar-**
450 **Henonin, L., Schmid, M., Weigel, D., Carter, D.E., Marchand, T., Risseeuw, E., Brogden, D.,**
451 **Zeko, A., Crosby, W.L., Berry, C.C., and Ecker, J.R.** (2003). Genome-wide insertional
452 mutagenesis of *Arabidopsis thaliana*. Science **301,** 653-657.
453 **Ayaydin, F., and Dasso, M.** (2004). Distinct in vivo dynamics of vertebrate SUMO paralogues.
454 Molecular Biology of the Cell **15,** 5208-5218.
455 **Baek, G.H., Cheng, H., Choe, V., Bao, X., Shao, J., Luo, S., and Rao, H.** (2013). Cdc48: a swiss army
456 knife of cell biology. Journal of Amino Acids **2013,** 183421.
457 **Bauer, J., Chen, K., Hiltbunner, A., Wehrli, E., Eugster, M., Schnell, D., and Kessler, F.** (2000). The
458 major protein import receptor of plastids is essential for chloroplast biogenesis. Nature **403,**
459 203-207.
460 **Beauclair, G., Bridier-Nahmias, A., Zagury, J.F., Saib, A., and Zamborlini, A.** (2015). JASSA: a
461 comprehensive tool for prediction of SUMOylation sites and SIMs. Bioinformatics **31,** 3483-
462 3491.
463 **Berardini, T.Z., Reiser, L., Li, D., Mezheritsky, Y., Muller, R., Strait, E., and Huala, E.** (2015). The
464 Arabidopsis information resource: Making and mining the "gold standard" annotated
465 reference plant genome. Genesis **53,** 474-485.
466 **Bergink, S., Ammon, T., Kern, M., Schermelleh, L., Leonhardt, H., and Jentsch, S.** (2013). Role of
467 Cdc48/p97 as a SUMO-targeted segregase curbing Rad51-Rad52 interaction. Nature Cell
468 Biology **15,** 526-532.

469 **Chang, C.C., Tung, C.H., Chen, C.W., Tu, C.H., and Chu, Y.W.** (2018). SUMOgo: Prediction of
470 sumoylation sites on lysines by motif screening models and the effects of various post-
471 translational modifications. Scientific Reports **8,** 15512.
472 **Citovsky, V., Lee, L.Y., Vyas, S., Glick, E., Chen, M.H., Vainstein, A., Gafni, Y., Gelvin, S.B., and Tzfira,**
473 **T.** (2006). Subcellular localization of interacting proteins by bimolecular fluorescence
474 complementation *in planta*. Journal of Molecular Biology **362,** 1120-1131.
475 **Clough, S.J., and Bent, A.F.** (1998). Floral dip: a simplified method for *Agrobacterium*-mediated
476 transformation of *Arabidopsis thaliana*. Plant Journal **16,** 735-743.
477 **Desterro, J.M., Rodriguez, M.S., and Hay, R.T.** (1998). SUMO-1 modification of IkappaBalpha inhibits
478 NF-kappaB activation. Molecular Cell **2,** 233-239.
479 **Elrouby, N., and Coupland, G.** (2010). Proteome-wide screens for small ubiquitin-like modifier
480 (SUMO) substrates identify Arabidopsis proteins implicated in diverse biological processes.
481 Proceedings of the National Academy of Sciences of the United States of America **107,**
482 17415-17420.
483 **Flores-Pérez, Ú., and Jarvis, P.** (2017). Isolation and suborganellar fractionation of Arabidopsis
484 chloroplasts. Methods in Molecular Biology **1511,** 45-60.
485 **Grimmer, J., Helm, S., Dobritzsch, D., Hause, G., Shema, G., Zahedi, R.P., and Baginsky, S.** (2020).
486 Mild proteasomal stress improves photosynthetic performance in Arabidopsis chloroplasts.
487 Nature Communications **11,** 1662.
488 **Hilgarth, R.S., and Sarge, K.D.** (2005). Detection of sumoylated proteins. Methods in Molecular
489 Biology **301,** 329-338.
490 **Hirsch, S., Muckel, E., Heemeyer, F., von Heijne, G., and Soll, J.** (1994). A receptor component of the
491 chloroplast protein translocation machinery. Science **266,** 1989-1992.
492 **Huang, W.H., Ling, Q.H., Bedard, J., Lilley, K., and Jarvis, P.** (2011). In vivo analyses of the roles of
493 essential Omp85-related proteins in the chloroplast outer envelope membrane. Plant
494 Physiology **157,** 147-159.
495 **Inaba, T., Alvarez-Huerta, M., Li, M., Bauer, J., Ewers, C., Kessler, F., and Schnell, D.J.** (2005).
496 Arabidopsis Tic110 is essential for the assembly and function of the protein import
497 machinery of plastids. Plant Cell **17,** 1482-1496.
498 **Jarvis, P.** (2008). Targeting of nucleus-encoded proteins to chloroplasts in plants. New Phytologist
499 **179,** 257-285.
500 **Jarvis, P., and Lopez-Juez, E.** (2013). Biogenesis and homeostasis of chloroplasts and other plastids.
501 Nature Reviews Molecular Cell Biology **14,** 787-802.
502 **Jarvis, P., Chen, L.J., Li, H.M., Pete, C.A., Fankhauser, C., and Chory, J.** (1998). An *Arabidopsis*
503 mutant defective in the plastid general protein import apparatus. Science **282,** 100-103.
504 **Karimi, M., Inze, D., and Depicker, A.** (2002). GATEWAY vectors for *Agrobacterium*-mediated plant
505 transformation. Trends in Plant Science **7,** 193-195.
506 **Karimi, M., De Meyer, B., and Hilson, P.** (2005). Modular cloning in plant cells. Trends Plant Science
507 **10,** 103-105.
508 **Kasmati, A.R., Töpel, M., Patel, R., Murtaza, G., and Jarvis, P.** (2011). Molecular and genetic
509 analyses of Tic20 homologues in *Arabidopsis thaliana* chloroplasts. Plant Journal **66,** 877-
510 889.
511 **Kessler, F., Blobel, G., Patel, H.A., and Schnell, D.J.** (1994). Identification of two GTP-binding
512 proteins in the chloroplast protein import machinery. Science **266,** 1035-1039.
513 **Kovacheva, S., Bedard, J., Patel, R., Dudley, P., Twell, D., Rios, G., Koncz, C., and Jarvis, P.** (2005). *In*
514 *vivo* studies on the roles of Tic110, Tic40 and Hsp93 during chloroplast protein import. Plant
515 Journal **41,** 412-428.
516 **Kurepa, J., Walker, J.M., Smalle, J., Gosink, M.M., Davis, S.J., Durham, T.L., Sung, D.Y., and Vierstra,**
517 **R.D.** (2003). The small ubiquitin-like modifier (SUMO) protein modification system in
518 Arabidopsis. Accumulation of SUMO1 and -2 conjugates is increased by stress. Journal of
519 Biological Chemistry **278,** 6862-6872.

520 **Lee, S., Lee, D.W., Lee, Y., Mayer, U., Stierhof, Y.D., Jurgens, G., and Hwang, I.** (2009). Heat shock
521 protein cognate 70-4 and an E3 ubiquitin ligase, CHIP, mediate plastid-destined precursor
522 degradation through the ubiquitin-26S proteasome system in *Arabidopsis*. Plant Cell **21,**
523 3984-4001.
524 **Lee, Y.J., Kim, D.H., Kim, Y.W., and Hwang, I.** (2001). Identification of a signal that distinguishes
525 between the chloroplast outer envelope membrane and the endomembrane system in vivo.
526 Plant Cell **13,** 2175-2190.
527 **Liebelt, F., and Vertegaal, A.C.** (2016). Ubiquitin-dependent and independent roles of SUMO in
528 proteostasis. American Journal of Physiology Cell Physiology **311,** C284-C296.
529 **Ling, Q., and Jarvis, P.** (2015). Regulation of chloroplast protein import by the ubiquitin E3 ligase SP1
530 is important for stress tolerance in plants. Current Biology **25,** 2527-2534.
531 **Ling, Q., Huang, W., and Jarvis, P.** (2011). Use of a SPAD-502 meter to measure leaf chlorophyll
532 concentration in Arabidopsis thaliana. Photosynthesis Research **107,** 209-214.
533 **Ling, Q., Huang, W., Baldwin, A., and Jarvis, P.** (2012). Chloroplast biogenesis is regulated by direct
534 action of the ubiquitin-proteasome system. Science **338,** 655-659.
535 **Ling, Q., Broad, W., Trösch, R., Töpel, M., Demiral Sert, T., Lymperopoulos, P., Baldwin, A., and**
536 **Jarvis, R.P.** (2019). Ubiquitin-dependent chloroplast-associated protein degradation in
537 plants. Science **363**.
538 **Miura, K., Rus, A., Sharkhuu, A., Yokoi, S., Karthikeyan, A.S., Raghothama, K.G., Back, D., Koo, Y.D.,**
539 **Jin, J.B., Bressan, R.A., Yun, D.J., and Hasegawa, P.M.** (2005). The Arabidopsis SUMO E3
540 ligase SIZ1 controls phosphate deficiency responses Proceedings of the National Academy of
541 Sciences of the United States of America **102,** 9734-9734.
542 **Nie, M., Aslanian, A., Prudden, J., Heideker, J., Vashisht, A.A., Wohlschlegel, J.A., Yates, J.R., and**
543 **Boddy, M.N.** (2012). Dual recruitment of Cdc48 (p97)-Ufd1-Npl4 ubiquitin-selective
544 segregase by small ubiquitin-like modifier protein (SUMO) and ubiquitin in SUMO-targeted
545 ubiquitin ligase-mediated genome stability functions. Journal of Biological Chemistry **287,**
546 29610-29619.
547 **Perry, S.E., and Keegstra, K.** (1994). Envelope membrane proteins that interact with chloroplastic
548 precursor proteins. Plant Cell **6,** 93-105.
549 **Saracco, S.A., Miller, M.J., Kurepa, J., and Vierstra, R.D.** (2007). Genetic analysis of SUMOylation in
550 Arabidopsis: conjugation of SUMO1 and SUMO2 to nuclear proteins is essential. Plant
551 Physiology **145,** 119-134.
552 **Schneider, C.A., Rasband, W.S., and Eliceiri, K.W.** (2012). NIH Image to ImageJ: 25 years of image
553 analysis. Nature Methods **9,** 671-675.
554 **Schnell, D.J., Kessler, F., and Blobel, G.** (1994). Isolation of components of the chloroplast protein
555 import machinery. Science **266,** 1007-1012.
556 **Shanmugabalaji, V., Chahtane, H., Accossato, S., Rahire, M., Gouzerh, G., Lopez-Molina, L., and**
557 **Kessler, F.** (2018). Chloroplast biogenesis controlled by DELLA-TOC159 interaction in early
558 plant development. Current Biology **28,** 2616-2623 e2615.
559 **Sowden, R.G., Watson, S.J., and Jarvis, P.** (2018). The role of chloroplasts in plant pathology. Essays
560 in Biochemistry **62,** 21-39.
561 **Sriramachandran, A.M., and Dohmen, R.J.** (2014). SUMO-targeted ubiquitin ligases. Biochimica et
562 Biophysica Acta **1843,** 75-85.
563 **Tranel, P.J., Froehlich, J., Goyal, A., and Keegstra, K.** (1995). A component of the chloroplastic
564 protein import apparatus is targeted to the outer envelope membrane via a novel pathway.
565 The EMBO Journal **14,** 2436-2446.
566 **Tzfira, T., Tian, G.W., Lacroix, B., Vyas, S., Li, J., Leitner-Dagan, Y., Krichevsky, A., Taylor, T.,**
567 **Vainstein, A., and Citovsky, V.** (2005). pSAT vectors: a modular series of plasmids for
568 autofluorescent protein tagging and expression of multiple genes in plants. Plant Molecular
569 Biology **57,** 503.

570 **van den Burg, H.A., Kini, R.K., Schuurink, R.C., and Takken, F.L.W.** (2010). *Arabidopsis* small
571 ubiquitin-like modifier paralogs have distinct functions in development and defense. Plant
572 Cell **22,** 1998-2016.
573 **Watson, S.J., Sowden, R.G., and Jarvis, P.** (2018). Abiotic stress-induced chloroplast proteome
574 remodelling: a mechanistic overview. Journal of Experimental Botany **69,** 2773-2781.
575 **Wu, F.H., Shen, S.C., Lee, L.Y., Lee, S.H., Chan, M.T., and Lin, C.S.** (2009). Tape-Arabidopsis Sandwich
576 - a simpler Arabidopsis protoplast isolation method. Plant Methods **5,** 16.
577 **Zhao, Q., Xie, Y., Zheng, Y., Jiang, S., Liu, W., Mu, W., Liu, Z., Zhao, Y., Xue, Y., and Ren, J.** (2014).
578 GPS-SUMO: a tool for the prediction of sumoylation sites and SUMO-interaction motifs.
579 Nucleic Acids Research **42,** W325-W330.

580 # Acknowledgements

581 We are very grateful to Alistair Haslam for initiating the genetic experiments. We also thank Dr Errin
582 Johnson and Raman Dhaliwal (Dunn School of Pathology, University of Oxford) for assistance with
583 the electron microscopy, and Prof Jane Langdale for advice during the course of the work. We are
584 grateful to Pedro Bota and Rita Ross for technical support. This work was supported by the Oxford
585 Interdisciplinary Bioscience Doctoral Training Partnership (DTP), and by grants from the
586 Biotechnology and Biological Sciences Research Council (BBSRC) (grant numbers BB/K018442/1,
587 BB/N006372/1, BB/R016984/1 and BB/R009333/1) to RPJ.

588 # Competing interests

589 The authors declare no competing interests.

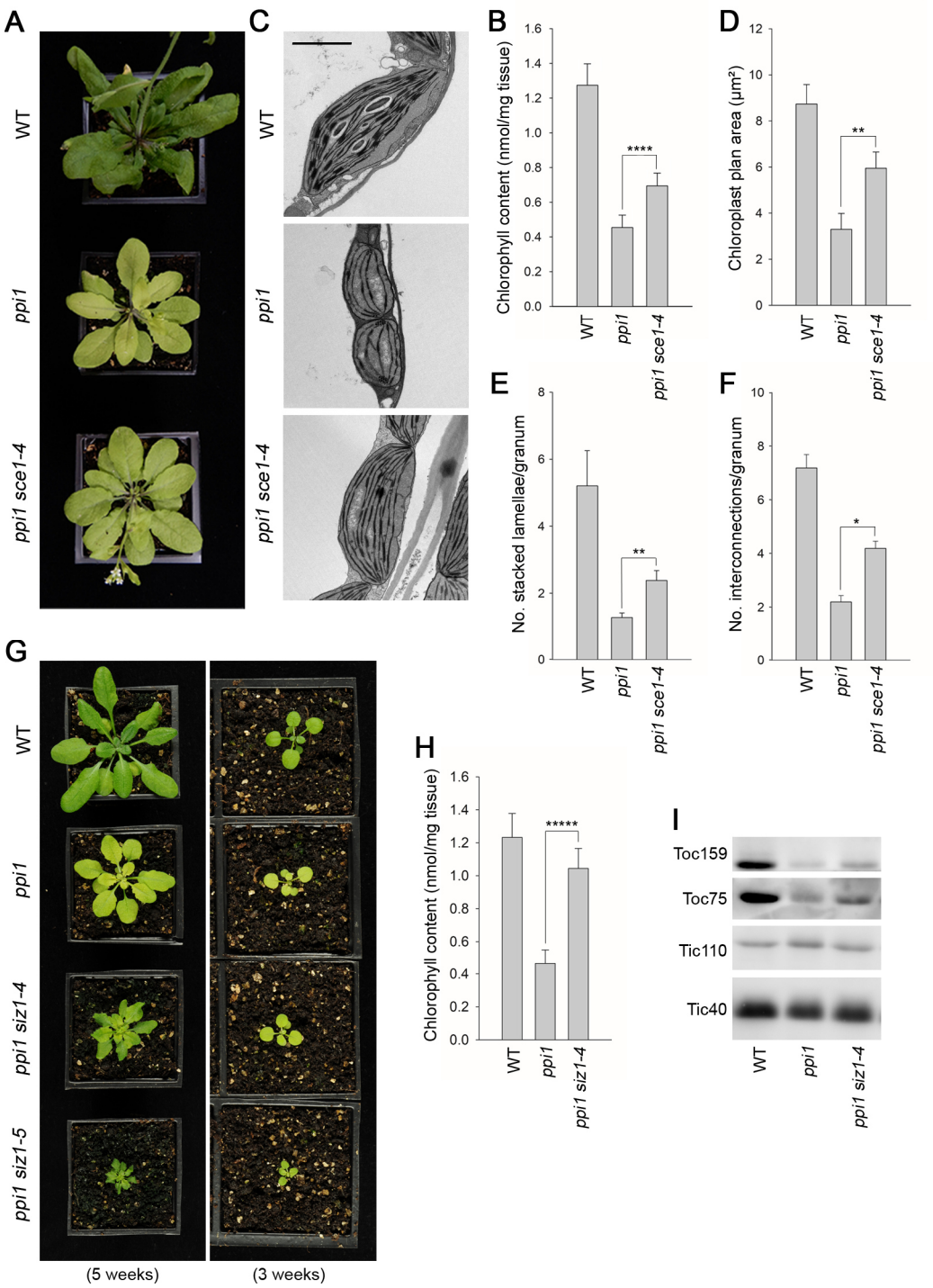

Figure 1

The E2 SUMO conjugating enzyme mutation, *sce1-4*, and the E3 SUMO ligase mutation, *siz1-4*, suppress the phenotype of plastid protein import mutant, *ppi1*.

(A) The *ppi1 sce1-4* double mutant appeared greener than *ppi1* after approximately five weeks of growth on soil.

(B) The *ppi1 sce1-4* double mutant showed enhanced accumulation of chlorophyll relative to *ppi1* after approximately five weeks of growth on soil. Measurements were taken from the plants shown in (A) on the day of photography, as well as additional similar plants. Error bars indicate standard

599 deviation from the mean (*n* = 7). There were significant differences between the *ppi1* and *ppi1 sce1-*
600 *4* plants (Two-tailed t-test, unpaired samples, T = 6.15, *p* = 0.000049).

601 (C) Transmission electron microscopy revealed improved chloroplast development in mature rosette
602 leaf mesophyll tissue of *ppi1 sce1-4* plants relative to *ppi1*. Plants that had been grown on soil for
603 approximately four weeks were analysed, and representative images are shown. Scale bar = 2 µm.

604 (D) Chloroplast plan area was elevated in *ppi1 sce1-4* relative to *ppi1*. The transmission electron
605 microscopy dataset was quantified. Error bars indicate standard deviation from the mean (*n* = 3
606 biological replicates). There were significant differences between the *ppi1* and *ppi1 sce1-4* plants
607 (Two-tailed t-test, unpaired samples, T = 4.65, *p* = 0.009674).

608 (E) Thylakoid membrane stacking was increased in *ppi1 sce1-4* relative to *ppi1*. The number of
609 stacked thylakoidal lamellae per granum was analysed. Error bars indicate standard error from the
610 mean (*n* = 3 biological replicates). There were significant differences between the *ppi1* and *ppi1*
611 *sce1-4* plants (Two-tailed t-test, unpaired samples, T = 5.53, *p* = 0.005221).

612 (F) Thylakoid membrane interconnections were increased in *ppi1 sce1-4* relative to *ppi1*. The
613 number of stromal thylakoidal lamellae emanating from each granum (granal interconnections) was
614 analysed. Error bars indicate standard error from the mean (*n* = 3 biological replicates). There were
615 significant differences between the *ppi1* and *ppi1 sce1-4* plants (Two-tailed t-test, unpaired samples,
616 T = 3.38, *p* = 0.0277).

617 (G) The *ppi1 siz1-4* and *ppi1 siz1-5* double mutants appeared greener than *ppi1* after different
618 periods of growth on soil. The plants were photographed after three weeks of growth (right panel)
619 and then again after five weeks of growth (left panel).

620 (H) The *ppi1 siz1-4* double mutant showed enhanced accumulation of chlorophyll relative to *ppi1*
621 after approximately five weeks of growth on soil. Measurements were taken from the plants shown
622 in (G) on the day of photography, as well as additional similar plants. Error bars indicate standard
623 deviation from the mean (*n* = 8). There were significant differences between the *ppi1* and *ppi1 siz1-4*
624 plants (Two-tailed t-test, unpaired samples, T = 11.01, *p* < 0.00001).

625 (I) TOC protein accumulation is improved in *ppi1 siz1-4* relative to *ppi1*. Analysis of the levels of
626 Toc75 and Toc159 in *ppi1 siz1-4* and relevant control plants was conducted by immunoblotting.
627 Protein samples were taken from the rosette tissue of plants that had been grown on soil for
628 approximately five weeks. Toc159 typically migrates as a complex series of bands owing to its
629 proteolytic sensitivity, and only the major band is shown. The TIC-associated proteins, Tic110 and
630 Tic40, were employed as controls.

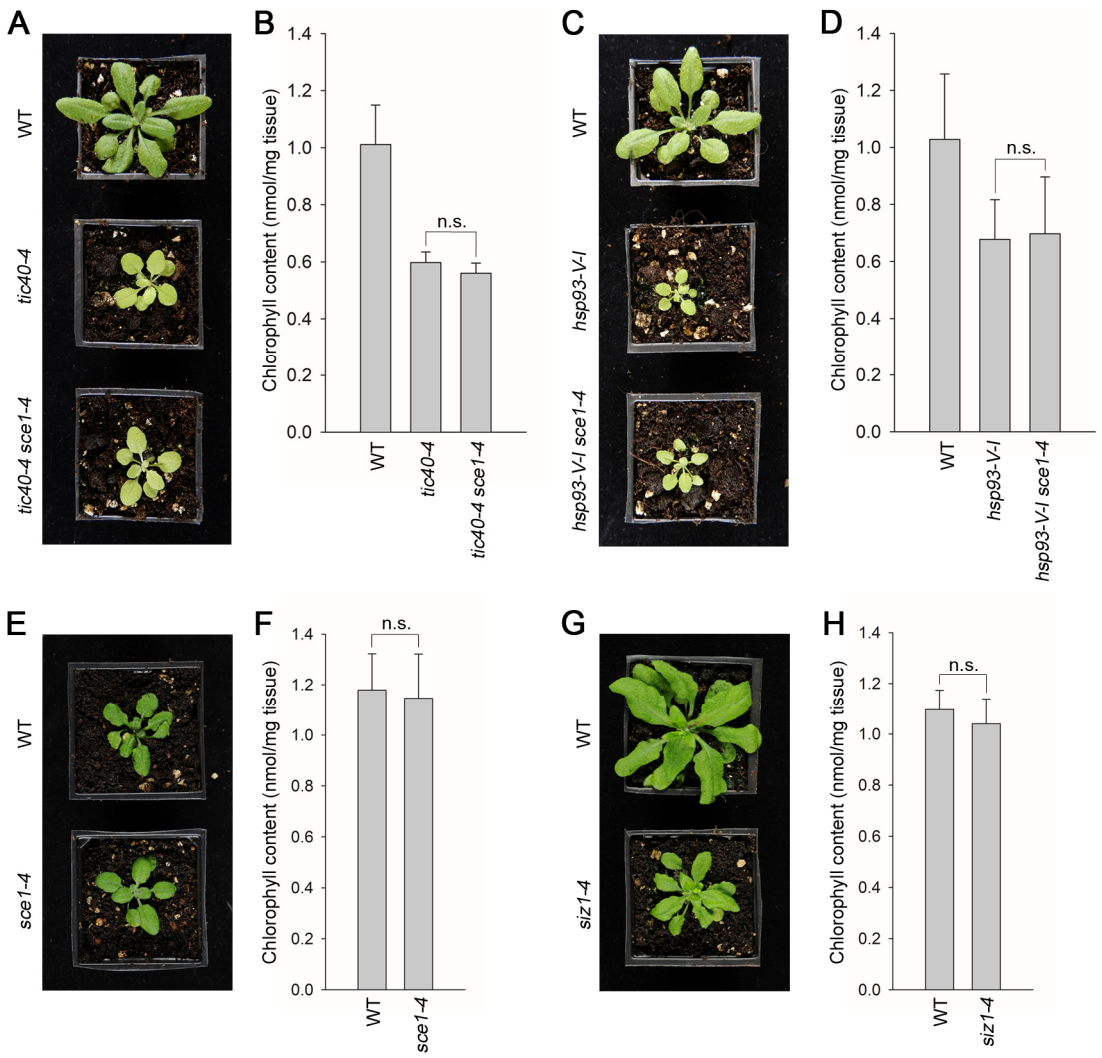

Figure 2

Genetic analysis reveals specificity of the suppression mediated by the *sce1-4* and *siz1-4* mutations.

(A) The *tic40-4 sce1-4* double mutant did not appear greener than *tic40-4* after approximately four weeks of growth on soil.

(B) The *tic40-4 sce1-4* double mutant did not show an enhanced accumulation of chlorophyll relative to *tic40-4* after approximately four weeks of growth on soil. Measurements were taken from the plants shown in (A) on the day of photography, as well as additional similar plants. Error bars indicate standard deviation from the mean (n = 3). There were no significant differences between the *tic40-4* and *tic40-4 sce1-4* plants (Two-tailed t-test, unpaired samples, T = 1.25, p = 0.280106).

(C) The *hsp93-V-I sce1-4* double mutant did not appear greener than *hsp93-V-I* after approximately four weeks of growth on soil.

(D) The *hsp93-V-I sce1-4* double mutant did not show an enhanced accumulation of chlorophyll relative to *hsp93-V-I* after approximately four weeks of growth on soil. Measurements were taken from the plants shown in (C) on the day of photography, as well as additional similar plants. Error bars indicate standard deviation from the mean (n = 5). There were no significant differences

648 between the *hsp93-V-I* and *hsp93-V-I sce1-4* plants (Two-tailed t-test, unpaired samples, T = 0.18, *p* =
649 0.860702).

650 (E) The *sce1-4* single mutant did not appear greener than wild-type plants after approximately four
651 weeks of growth on soil.

652 (F) The *sce1-4* single mutant did not show an enhanced accumulation of chlorophyll relative to wild-
653 type plants after approximately four weeks of growth on soil. Measurements were taken from the
654 plants shown in (E) on the day of photography, as well as additional similar plants. Error bars
655 indicate standard deviation from the mean (*n* = 7). There were no significant differences between
656 the *sce1-4* and wild type plants (Two-tailed t-test, unpaired samples, T = 0.38, *p* = 0.708484).

657 (G) The *siz1-4* single mutant did not appear greener than wild-type plants after approximately five
658 weeks of growth on soil.

659 (H) The *siz1-4* single mutant did not show an enhanced accumulation of chlorophyll relative to wild-
660 type plants after approximately five weeks of growth on soil. Measurements were taken from the
661 plants shown in (G) on the day of photography, as well as from additional similar plants. Error bars
662 indicate standard deviation from the mean (*n* = 4-5). There were no significant differences between
663 the *siz1-4* and wild type plants (T = 0.96, *p* = 0.370055).

664

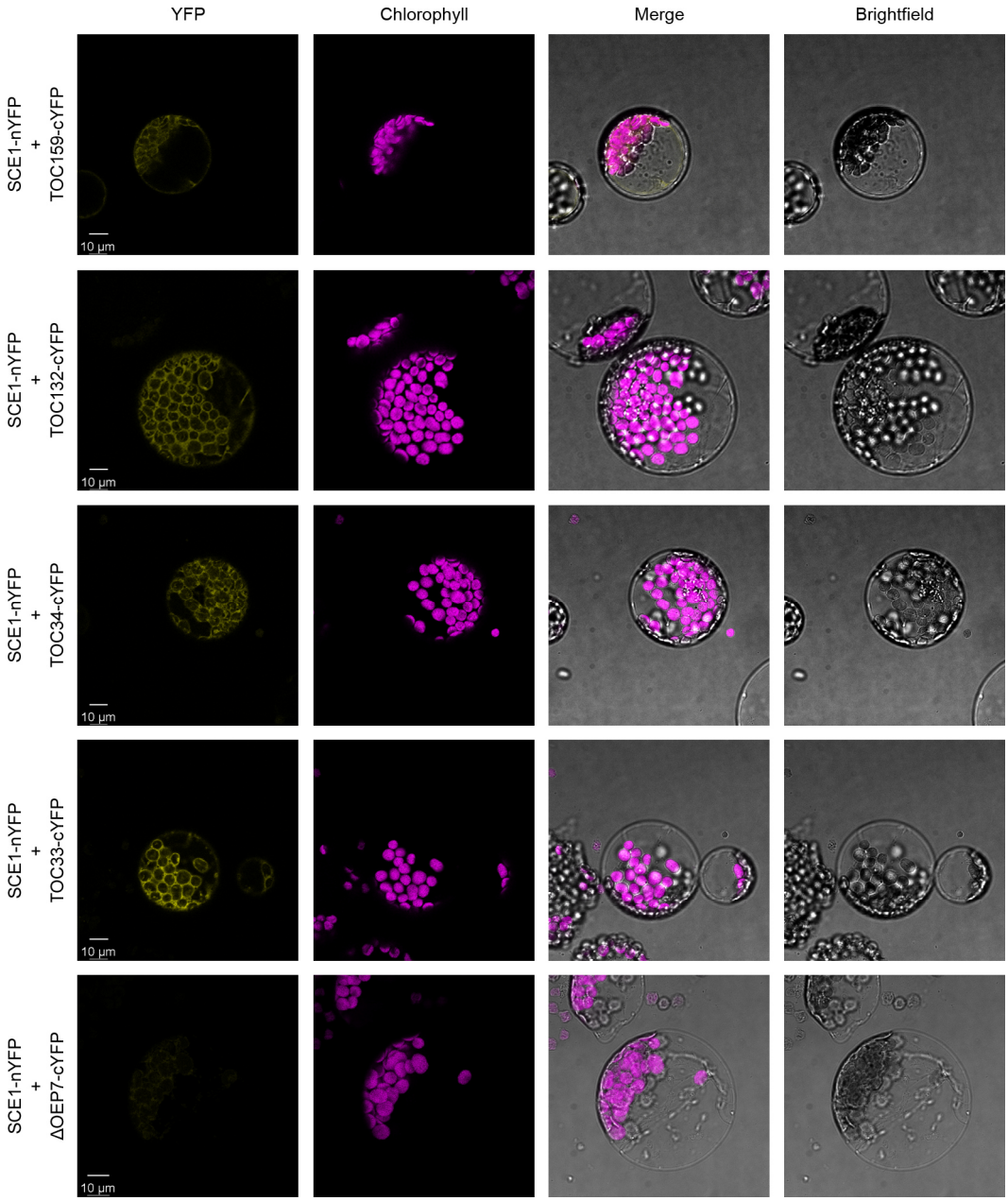

Figure 3

SCE1 physically interacts with TOC proteins *in vivo.*

Bimolecular fluorescence complementation (BiFC) analysis of SCE1 protein-protein interactions was performed by imaging *Arabidopsis* protoplasts co-expressing proteins fused to complementary N-terminal (nYFP) and C-terminal (cYFP) fragments of the YFP protein, as indicated. Chlorophyll autofluorescence images were employed to orientate the YFP signals in relation to the chloroplasts. In this analysis, SCE1 physically associated with TOC proteins. The images shown are representative confocal micrographs indicating associations between SCE1 and Toc159, Toc132, Toc34 and Toc33. In contrast, SCE1 did not physically associate with ΔOEP7-cYFP (comprising the transmembrane domain of OEP7, which is sufficient to direct targeting to the chloroplast outer envelope, fused to the cYFP fragment), which served as a negative control. Scale bars = 10 µm.

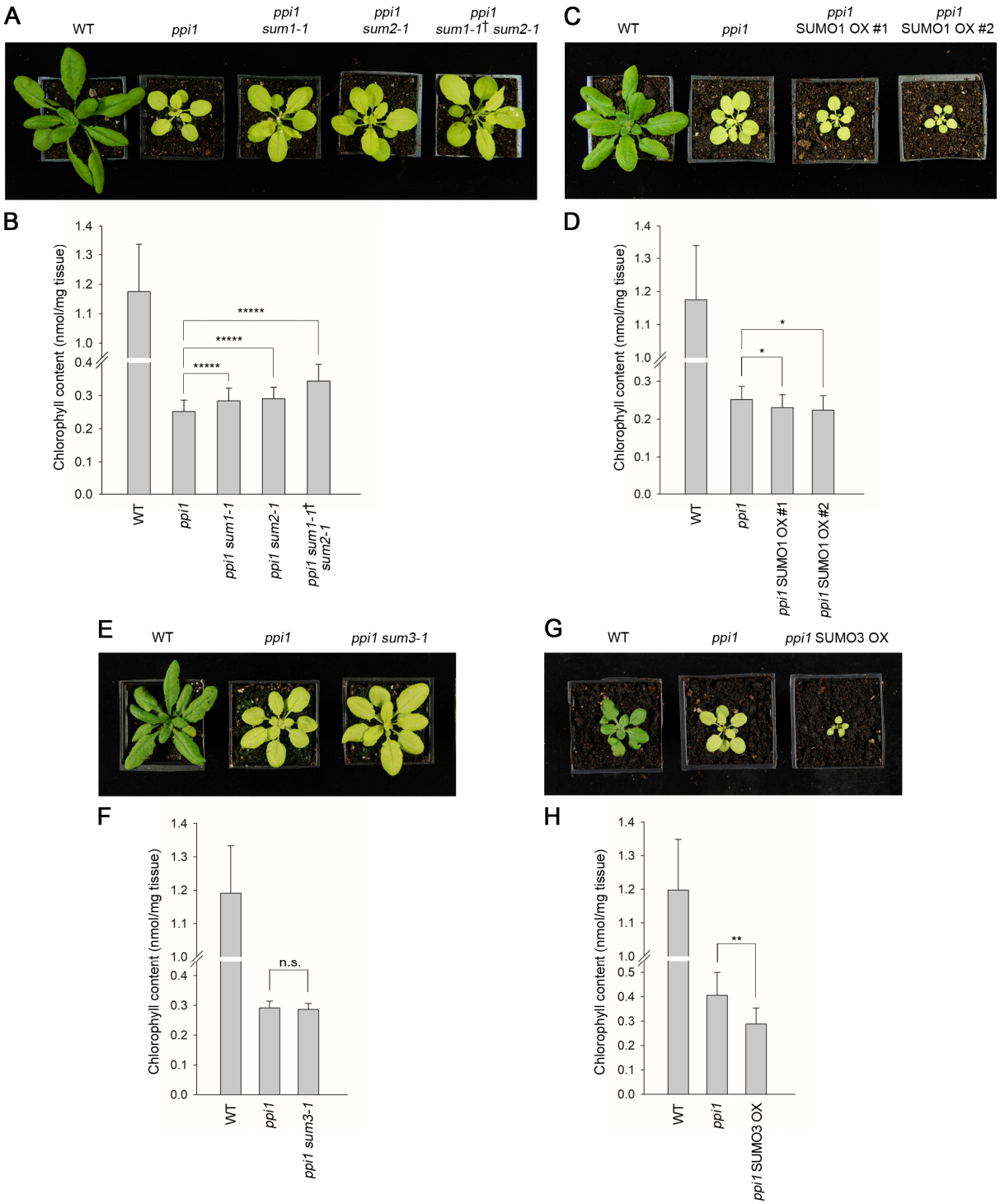

Figure 4

Genetic interactions between *ppi1* and the genes encoding three SUMO isoforms.

(A) The *ppi1 sum1-1, ppi1 sum2-1,* and *ppi1 sum1-1*† *sum2-1* double and triple mutants appeared greener than *ppi1* after approximately four weeks of growth on soil. The dagger symbol indicates that the triple mutant was heterozygous with respect to the *sum1-1* mutation.

(B) The *ppi1 sum1-1, ppi1 sum2-1,* and *ppi1 sum1-1*† *sum2-1* double and triple mutants showed enhanced accumulation of chlorophyll relative to *ppi1* after approximately four weeks of growth on soil. Measurements were taken from the plants shown in (A) on the day of photography, as well as

686 additional similar plants. Error bars indicate standard deviation from the mean (n = 20-71). There
687 were significant differences between the samples, as measured via a one-way ANOVA (F = 26.21, p =
688 6.65×10^{-14}). A post-hoc Tukey HSD test indicated that there was a significant difference between
689 the *ppi1* and *ppi1 sum1-1* samples ($p < 0.00001$). There were also significant differences between the
690 *ppi1* and *ppi1 sum2-1* samples ($p < 0.00001$), and between the *ppi1* and *ppi1 sum1-1* sum2-1*
691 samples ($p < 0.00001$).

692 (C) The *ppi1* SUMO1 overexpression (OX) lines appeared smaller and paler than *ppi1* after
693 approximately four weeks of growth on soil.

694 (D) The *ppi1* SUMO1 OX lines showed reduced accumulation of chlorophyll relative to *ppi1* after
695 approximately four weeks of growth on soil. Measurements were taken from the plants shown in (C)
696 on the day of photography, as well as additional similar plants. Error bars indicate standard deviation
697 from the mean (n = 24-37). There were significant differences between the *ppi1* and *ppi1* SUMO1 OX
698 #1 plants (Two-tailed t-test, unpaired samples, T = 2.27, p = 0.026832), and between the *ppi1* and
699 *ppi1* SUMO1 OX #2 plants (Two-tailed t-test, unpaired samples, T = 2.49, p = 0.01634).

700 (E) The *ppi1 sum3-1* double mutant did not appear greener than *ppi1* after approximately four
701 weeks of growth on soil.

702 (F) The *ppi1 sum3-1* double mutant did not show an enhanced accumulation of chlorophyll relative
703 to *ppi1* after approximately four weeks of growth on soil. Measurements were taken from the plants
704 shown in (E) on the day of photography, as well as additional similar plants. Error bars indicate
705 standard deviation from the mean (n = 10). There were no significant differences between the *ppi1*
706 and *ppi1 sum3-1* plants (Two-tailed t-test, unpaired samples, T = 0.54, p = 0.59407).

707 (G) The *ppi1* SUMO3 overexpression line appeared smaller and paler than *ppi1* after approximately
708 three weeks of growth on soil.

709 (H) The *ppi1* SUMO3 overexpression line showed reduced accumulation of chlorophyll relative to
710 *ppi1* after approximately three weeks of growth on soil. Measurements were taken from the plants
711 shown in (G) on the day of photography, as well as additional similar plants. Error bars indicate
712 standard deviation from the mean (n = 8-10). There were significant differences between the *ppi1*
713 SUMO3 OX plants and *ppi1* (Two-tailed t-test, unpaired samples, T = 2.99, p = 0.008688).

714

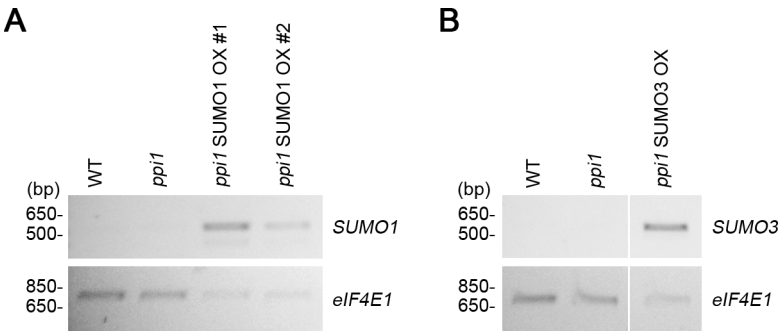

Figure 4 supplement

Analysis of the expression of the 35S:*SUMO1* and 35S:*SUMO3* transgenes in the selected transformants by RT-PCR.

Total RNA was extracted from the rosette tissue of plants that had been grown on soil for approximately four weeks. The expression of *SUMO1* (A) or *SUMO3* (B), and of the control gene, *eIF4E1*, was analysed by semi-quantitative RT-PCR. A limited number of amplification cycles (n = 26) was employed to prevent saturation. Migration positions of standards are displayed to the left of the gel images.

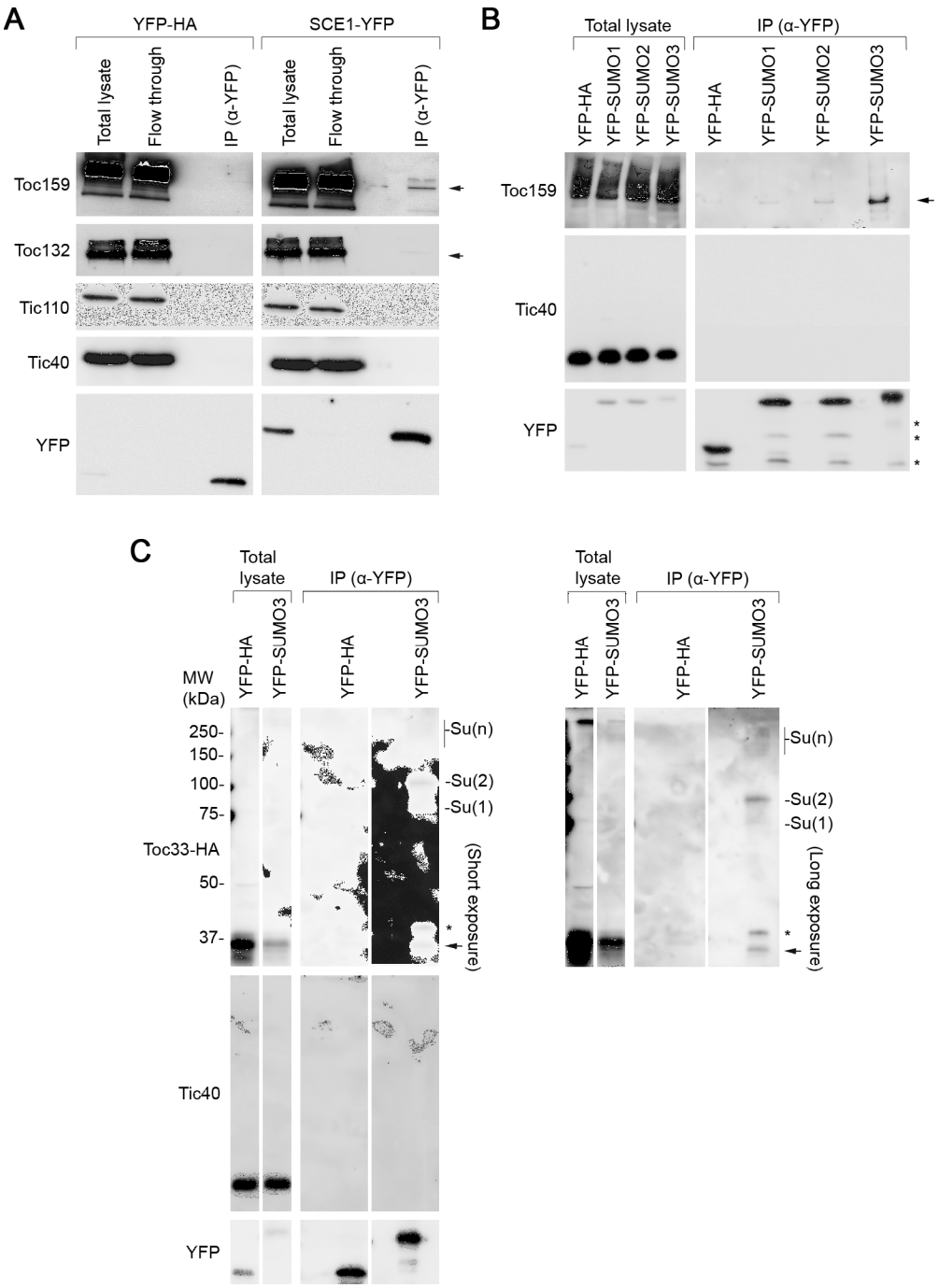

Figure 5

Immunoprecipitation analysis reveals that TOC proteins are SUMO targets.

(A) SCE1 physically associated with native TOC proteins. *Arabidopsis* protoplasts expressing YFP-HA (left panel) or SCE1-YFP (right panel) were solubilised and subjected to immunoprecipitation (IP) analysis. The YFP-HA construct served as a negative control. In both cases, three samples were analysed: The 'Total lysate' sample (total protein extract from solubilised protoplasts); the 'Flow through' sample (the total protein sample after incubation with anti-YFP beads); and the 'IP' sample (the eluted fraction of the total protein sample that bound to the anti-YFP beads). The samples were analysed by immunoblotting, revealing that SCE1-YFP, but not the YFP-HA control, was associated with native Toc159 and Toc132 (indicated by the two arrows). Neither SCE1-YFP nor YFP-HA was associated with native Tic110 or Tic40, which were employed as negative control proteins.

737 (B) All three SUMO isoforms physically associated with native Toc159. Protoplasts expressing YFP-
738 HA, YFP-SUMO1, YFP-SUMO2 or YFP-SUMO3 were solubilised and subjected to IP analysis as in (A).
739 In all four cases, two samples (the 'Total lysate' and the 'IP' samples) were analysed by
740 immunoblotting. Toc159 was resolved on an 8% acrylamide gel for four hours to maximise the
741 resolution of high molecular weight bands. All three YFP-SUMO proteins were found to associate
742 with native Toc159 (indicated by the arrow); however, YFP-SUMO3 immunoprecipitated Toc159 with
743 the greatest efficiency. Analysis of a long exposure of the YFP blot revealed the presence of high
744 molecular weight bands, for all three YFP-SUMO fusion proteins, consistent with the formation of
745 SUMO conjugates. None of the four YFP fusion proteins associated with native Tic40, which served
746 as a negative control protein. The asterisks indicate non-specific bands.

747 (C) YFP-SUMO3 physically associated with Toc33-HA and related high molecular weight species.
748 Protoplasts co-expressing YFP-SUMO3 or YFP-HA together with Toc33-HA were solubilised and
749 subjected to IP analysis as in (A). In both cases, two samples (the 'Total lysate' and 'IP' samples) were
750 analysed by immunoblotting. The results showed that YFP-SUMO3, but not YFP-HA, was associated
751 with Toc33-HA (indicated by the arrow). Bands corresponding to the molecular weight of Toc33-HA
752 bearing one, two or several YFP-SUMO3 motifs were also detected on the membrane (indicated as
753 Su(1), Su(2), and Su(n)). The predicted molecular weight of YFP-SUMO3 is approximately 38.9 kDa.
754 Neither YFP-SUMO3 nor YFP-HA was associated with Tic40, which served as a negative control
755 protein. The asterisk indicates a nonspecific band.

756

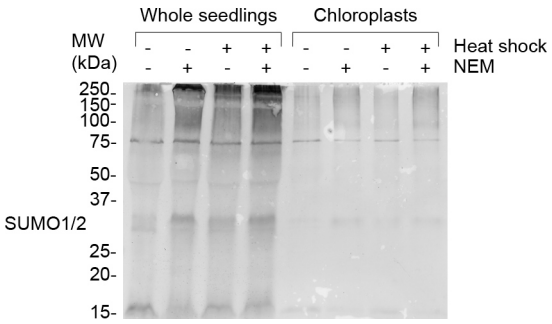

Figure 5 supplement 1

Chloroplast resident proteins are SUMOylated.

Anti-SUMO1 immunoblot analysis of protein samples taken from whole seedlings (left hand side) and isolated chloroplasts (right hand side). Where indicated, the samples were exposed to heat shock (42°C for 30 seconds) and/or incubated with 10 mM NEM to aid the detection of SUMOylated proteins. The anti-SUMO1 antibody used is known to show significant cross-reactivity with SUMO2 (Kurepa et al., 2003).

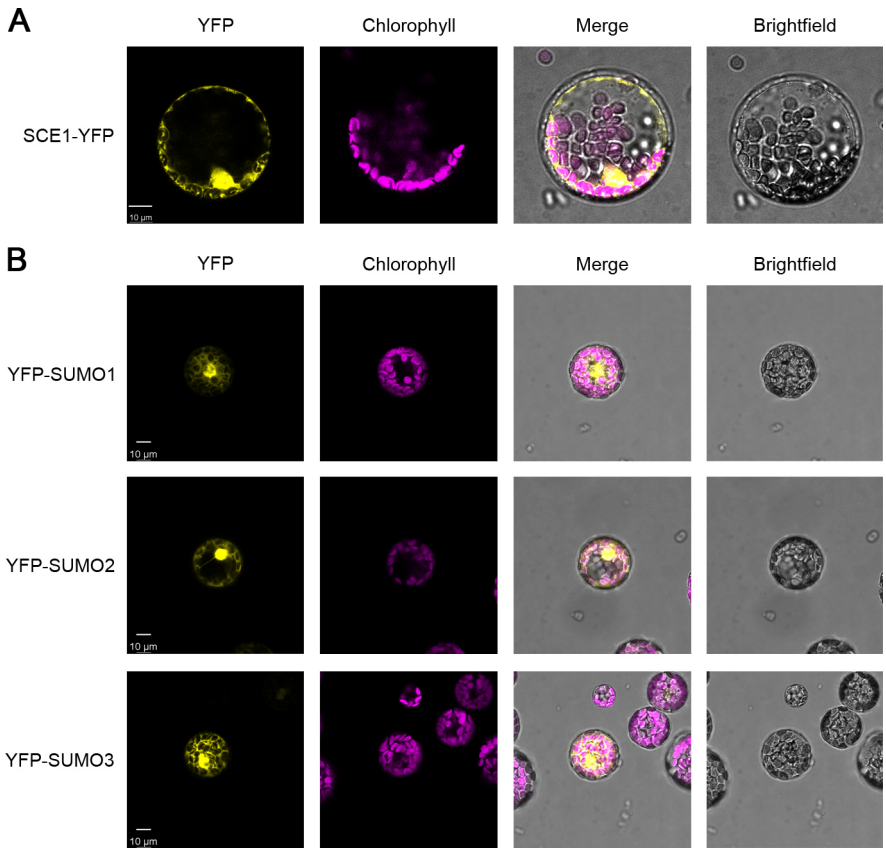

Figure 5 supplement 2

Analysis of the expression of the YFP-tagged constructs used in the immunoprecipitation experiments by confocal microscopy.

The expression of the SCE1-YFP construct (A), and of the three YFP-SUMO constructs (B), was analysed and confirmed by imaging transfected *Arabidopsis* protoplasts. Chlorophyll autofluorescence images were employed to orientate the YFP signals in relation to the chloroplasts. Representative confocal micrographs show a typical protoplast in each case. Scale bars = 10 µm.

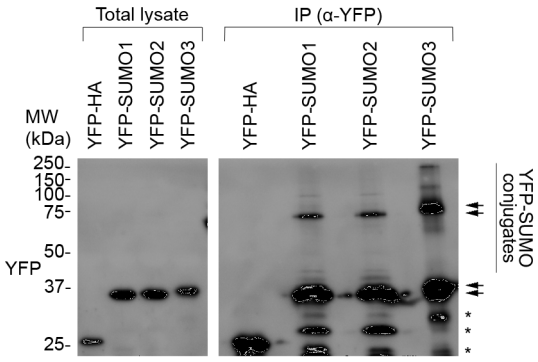

774

775 **Figure 5 supplement 3**

776 **All three YFP-SUMO probes are conjugation-competent.**

777 The membrane shown is the same as the one presented in Figure 5B (YFP panel). In this case, the
778 membrane was visualised using a long exposure to aid the detection of weakly abundant protein
779 bands. As well as the YFP-SUMO monomers, additional high molecular bands and smears were seen
780 in the IP samples, indicating the capture of large numbers of SUMOylated proteins. This shows that
781 all three YFP-SUMO probes could be successfully conjugated, as expected (Ayaydin and Dasso,
782 2004). The positions of the YFP-SUMO monomers (lower pair of arrows), and of the various SUMO
783 adducts (vertical bar) potentially including di-SUMO (upper pair of arrows), are indicated. Note that
784 YFP-SUMO3 migrated more slowly than the other two fusions, as expected. The asterisks indicate
785 non-specific bands.

786

787 **Table 1**

788 **Bioinformatic analysis predicts that the core TOC proteins in *Arabidopsis* contain SUMOylation**
789 **sites and SUMO interaction motifs.**

790 The GPS-SUMO algorithm was applied to the amino acid sequences of Toc159, Toc132, Toc120,
791 Toc90, Toc75, Toc33 and Toc34 using the 'high stringency' setting, and the results generated are
792 shown in columns 2, 3 and 4. 'Consensus' sites fall within canonical SUMO site motifs: ψ-K-X-E
793 (where ψ indicates a hydrophobic amino acid, and X indicates any amino acid residue). 'Non-
794 consensus' sites do not fall within canonical SUMO site motifs; analysis shows that ~40% of
795 SUMOylation may occur at non-consensus sites (Zhao et al., 2014). 'SUMO Interaction' sites are
796 predicted to mediate the non-covalent interaction between proteins and SUMO peptides. The JASSA
797 algorithm was also applied to the amino acid sequences using the 'high cut-off' setting (see column
798 5). aa denotes amino acids.

799

Protein name	Position (aa)	*p*-value	Type	Also predicted by JASSA (high stringency)?
atToc159	95	0.021	Consensus	No
(At4g02510)	106	0.034	Consensus	Yes
1503 aa	126	0.032	Consensus	Yes
	144	0.02	Consensus	Yes
	151	0.02	Consensus	No
	246-250	0.005	SUMO Interaction	Yes
	408-412	0.009	SUMO Interaction	Yes
	486-490	0.009	SUMO Interaction	Yes
	498	0.022	Consensus	No
	502	0.049	Non-consensus	No
	539	0.026	Consensus	No
	1300	0.049	Non-consensus	No
	1370	0.01	Consensus	Yes
atToc132	30	0.006	Consensus	Yes
(At2g16640)	66	0.036	Consensus	Yes
1206 aa	352	0.002	Consensus	No
	895	0.005	Consensus	No
	1077	0.014	Consensus	No
atToc120	52	0.008	Consensus	No
(At3g16620)	57	0.031	Consensus	No
1084 aa	209	0.05	Non-consensus	No
	777	0.006	Consensus	No
	959	0.013	Consensus	No
atToc90	191	0.027	Consensus	Yes
(At5g20300)	481	0.017	Consensus	No
793 aa	711	0.02	Consensus	No
	786	0.042	Non-consensus	Yes

atToc75 (At3g46740) 818 aa	434 513	0.049 0.029	Non-consensus Consensus	No No
atToc33 (At1g02280) 297 aa	291	0.044	Non-consensus	No
atToc34 (At5g05000) 313 aa	290 298	0.026 0.043	Consensus Non-consensus	No Yes

800

801

802 **Table 2**

803 **Primers used during the course of this study.**

804 (A) Primers used in restriction cloning procedures.

Primer name	Sequence*	Used to generate…
SCE1 F (HindIII)	AAAAGCTTATGGCTAGTGGAATCGCTC	pSAT4(A)-nEYFP-N1 SCE1
SCE1 R (EcoRI)	AAGAATTCGACAAGAGCAGGATACTGCTTG	pSAT4(A)-nEYFP-N1 SCE1
Toc159-5 F (EcoRI)	AAGAATTCAATGGACTCAAAGTCGGTT	pSAT4-cEYFP-C1-B Toc159
Toc159-3 R (SalI)	AAGTCGACTTAGTACATGCTGTACTT	pSAT4-cEYFP-C1-B Toc159
Toc132-5 F (XhoI)	AACTCGAGCTATG GGAGATGGGACTGAG	pSAT4-cEYFP-C1-B Toc132
Toc132-3 R (SmaI)	AACCCGGGTCATTGTCCATATTGCGT	pSAT4-cEYFP-C1-B Toc132
Toc33-5 F (HindIII)	AGAAGCTTCGATGGGGTCTCTCGTTCGT	pSAT4-cEYFP-C1-B Toc33
Toc33-3 R (XbaI)	AATCTAGATTAAAGTGGCTTTCCACT	pSAT4-cEYFP-C1-B Toc33
Toc34-5 F (HindIII)	AGAAGCTTCGATGGCAGCTTTGCAAACG	pSAT4-cEYFP-C1-B Toc34
Toc34-3 R (XbaI)	AATCTAGATCAAGACCTTCGACTTGC	pSAT4-cEYFP-C1-B Toc34
OEP7 F (XhoI)	CTCGAGATGGGAAAAACTTCGGGA	pSAT4(A)-cEYFP-N1 ΔOEP7
OEP7-35 R (KpnI)	GGTACCGGAATTTATCGAGGAAAGG	pSAT4(A)-cEYFP-N1 ΔOEP7
SFR2 F (KpnI)	GGTACCAACTAGAAAGATCCGGTG	pSAT4(A)-cEYFP-N1 SFR2
SFR2-ns R (XmaI)	CCCGGGGTCAAAGGGTGAGGCTAA	pSAT4(A)-cEYFP-N1 SFR2

805

806 (B) Primers used in Gateway cloning procedures.

Primer name	Sequence*	Used to generate…
SCE1 Gateway F	GGGGACAAGTTTGTACAAAAAAGCAGGCTCCATGGCTAGTGGAATCGCTC	p2GWY7 SCE1
SCE1 Gateway R	GGGGACCACTTTGTACAAGAAAGCTGGGTTGACAAGAGCAGGATACTGC	p2GWY7 SCE1
SUMO1 Gateway F	GGGGACAAGTTTGTACAAAAAAGCAGGCTCCTCTGCAAACCAGGAGGAAGACAAG	p2YGW7 SUMO1
SUMO1 Gateway R	GGGGACCACTTTGTACAAGAAAGCTGGGTTTCAGGCCGTAGCACCACC	p2YGWY SUMO1
SUMO2 Gateway F	GGGGACAAGTTTGTACAAAAAAGCAGGCTCCTCTGCTACTCCGGAAGAAGAC	p2YGW7 SUMO2
SUMO2 Gateway R	GGGGACCACTTTGTACAAGAAAGCTGGGTTCTAAAAGCAGAAGAGCTTCAGGCC	p2YGW7 SUMO2
SUMO3 Gateway F	GGGGACAAGTTTGTACAAAAAAGCAGGCTCCTCTAACCCTCAAGATGACAAGCCC	p2YGW7 SUMO3
SUMO3 Gateway R	GGGGACCACTTTGTACAAGAAAGCTGGGTTTTAAAGCCCATTATGATCGAAAAGC	p2YGW7 SUMO3

807

808 (C) Primers used in RT-PCR experiments.

Primer name	Sequence	Used to amplify…
SUMO1 F(2)	AAAAAGCAGGCTCCACAAAAGCCACGGCCAATTAG	*SUMO1*
SUMO1 R(2)	AGAAAGCTGGGTTCCATTCATATCACACACAAGCCC	*SUMO1*
SUMO3 F	ACAGACTGGAGTTTTTGTTTC	*SUMO3*
SUMO3 R	CTCATGAGTCATTTACACACACG	*SUMO3*
eIF4E1 F	AAGATTTGAGAGGTTTCAAGCGGTGTAAG	*eIF4E1*
eIF4E1 R	AAACAATGGCGGTAGAAGACACTC	*eIF4E1*

809

810 (D) Primers used to genotype mutants.

Primer name	Sequence	Used to genotype…
SUMO1 F(2)	AAAAAGCAGGCTCCACAAAAGCCACGGCCAATTAG	*sum1-1*

SUMO1 R(2)	AGAAAGCTGGGTTCCATTCATATCACACACAAGCCC	*sum1-1*
SUMO2 F	CGTTGTTGGTACTTGGTTGG	*sum2-1*
SUMO2 R	CAAAACTCTAAACTGGTCGG	*sum2-1*
SUMO3 F	ACAGACTGGAGTTTTTGTTTC	*sum3-1*
SUMO3 R	CTCATGAGTCATTTACACACACG	*sum3-1*
SCE1 F	CGCCGCGAAATCTGGACC	*sce1-4*
SCE1 R	TTCCTCTCTTCAGCTAAACG	*sce1-4*
SIZ1 F(2)	GCAAACAGGGAAAGAAGCAGG	*siz1-4*
SIZ1 R(2)	CATTGAGTCTGTTTCTAGCG	*siz1-4*
LBb1	GCGTGGACCGCTTGCTGCAACT	SALK lines (left border)
LB1	GCCTTTTCAGAAATGGATAAATAGCCTTGCTTCC	SAIL lines (left border)

811

812 * Restriction sequences are underlined.